

We are IntechOpen, the world's leading publisher of Open Access books Built by scientists, for scientists

4,800

Open access books available

122,000

International authors and editors

135M

Downloads

Our authors are among the

154

Countries delivered to

TOP 1%

most cited scientists

12.2%

Contributors from top 500 universities



WEB OF SCIENCE™

Selection of our books indexed in the Book Citation Index
in Web of Science™ Core Collection (BKCI)

Interested in publishing with us?
Contact book.department@intechopen.com

Numbers displayed above are based on latest data collected.
For more information visit www.intechopen.com



Remote Optical Diagnostics of Nonstationary Aerosol Media in a Wide Range of Particle Sizes

Olga Kudryashova et al.*

*Institute for Problems of Chemical and Energetic Technologies SB RAS
Russia*

1. Introduction

Polydisperse gas flows with condensed particles suspended therein are widely spread in nature and play an important role in many branches of the modern engineering and technology. There is a necessity for estimating parameters of disperse media in the manufacturing processes, scientific research, and atmosphere sounding. In industry, the result of this estimation can be employed as the quality measure of a product. When designing and distributing multi-phase systems to study the processes of controlling their parameters, it is also needed to determine values of the quantities characterizing such systems.

Technological processes exploit submicron media alongside with those of large and medium sizes. In such a system the particle sizes vary from tenths of nanometers to tenths of micrometers, and the resultant product may possess significantly different properties, even at small size variations of the condensed phase of a substance used. In this case, it becomes necessary to restore the particle size distribution function taking into account the contribution of all the particles present in the medium. Such functionality may be required from a measuring device when selecting modes of operation or designing sprayer units, controlling the quality of various micro- and nanopowders, monitoring the ecological situation of an area, and studying the dustiness of shop floors. Furthermore, the experimental information on disperse aerosol parameters is needed for evaluating the adequacy degree of a mathematical model accepted to describe an actual process and serves as initial data to calculate working processes in certain devices (Zuyev et al., 1986). The overview of the existing devices to investigate aerosol media has however shown that it cannot be realized using the known instruments.

The available techniques of determining the condensed phase dispersiveness can conditionally be divided into two main groups based on: (i) estimating the particle size in samples selected from a medium under examination and (ii) direct noncontact determination of sizes of the particles present in the medium. The sampling methods have gained a wide distribution, but the essential drawbacks of such methods are both the

* Anatoly Pavlenko, Boris Vorozhtsov, Sergey Titov, Vladimir Arkhipov, Sergey Bondarchuk, Eugeny Maksimenko, Igor Akhmadeev and Eugeny Muravlev
Institute for Problems of Chemical and Energetic Technologies SB RAS, Russia

introduction of disturbances into a medium under examination and the complexity of ensuring the representativeness of samples collected. To the noncontact methods of studying aerosols are optical techniques related (Table 1).

Method	Problems to solve	Peculiarities
Spectral transparency	Estimation of the distribution function and concentration. The size range of the measured particles when using the probe radiation of the visible spectrum is 0.01–30 μm .	Requires determining the transmission coefficient within a wavelength interval of $\lambda_{\min} \leq \lambda \leq \lambda_{\max}$ where about 20–30 measurements need to be conducted at equidistant values of λ . The technical implementation involves broad-spectrum optical radiation sources and selective detectors.
Small-angle scattering	Estimation of the distribution function without preliminary information on physical properties of a substance. When using a laser with a wavelength of 0.63 μm , the size range of the measured particles is 2–100 μm .	The method is very demanding of the accuracy in determining the scattering indicatrix; in this connection, the problem of restoring the particle size distribution function may be solved incorrectly. The technical implementation is relatively simple.
Complete indicatrix	Estimation of the distribution function. When a laser with a wavelength of 0.63 μm is used, the size range of the measured particles is 0.2–100 μm .	Requires measurements in the entire range of scattering angles.
Lidar	Evaluation of the microstructure of an aerosol.	The back scattering is very small. Requires the application of an high-sensitive radiation detector.

Table 1. The optical methods to study aerosols

The methods allow the high-speed characterization of a disperse medium directly during the process of its generation or evolution without introducing any changes into an object under study. Various values that are of interest to a researcher under the given process can be estimated from the change in the scattered, attenuated or reflected radiation passed through an aerosol (Arkhipov, 1987).

The main aerosol parameters are the condensed phase dispersiveness and its concentration. In order to measure simultaneously these characteristics in dynamics and consider the evolution process of an aerosol cloud as applied to media of a broad particle size range, it is necessary to employ several different methods combined into a unified measuring system. Following the analysis of the optical methods for measuring the aerosol dispersiveness, a decision was made to utilize the methods of small-angle scattering and spectral transparency. The chosen methods, mutually supplementing each other, permit (i) determining the dispersiveness of a nonsteady heterogeneous system with its high velocity

of travel, (ii) conducting measurements at significant background light, (iii) recording particles of diameters between hundreds of nanometers (the spectral transparency method) and several tenths of micrometers (the small-angle method), and (iv) using less detectors with the possibility of their remote location. When classically implemented, these methods however rely on solving the inverse problem that is incorrect and therefore require a modification in a part of both mathematical result treatment and instrumentation, to increase the informativeness of data obtainable from experiments.

2. Modified method of spectral transparency

The study into the disperse parameters of aerosol media containing 1–100 μm particles has led to a modified method of spectral transparency to measure the mean size and concentration. The method is based on measuring spectral coefficients of particle cloud-induced attenuation of laser radiation with a limited set of probe radiation wavelengths and on calculating averaged attenuation efficiency factors of radiation \bar{Q} (Vorozhtsov et al. 1997). This method does not make it possible to determine the particle size distribution function $f(D)$, but is suitable to measure mean particle sizes, particularly the mean volumetric-surface diameter D_{32} , because it has such merits as simple instrumentation and alignment and can diagnose high-temperature two-phase flows and other aerosol media of a high optical density.

The essence of this method consists in solving the inverse problem for the integral equation:

$$\tau_\lambda = \frac{\pi C_n l}{4} \int_0^\infty D^2 Q(D, \lambda, m) f(D) dD, \quad (1)$$

where τ_λ – the optical thickness; C_n – the calculated particle concentration; λ – the probe radiation wavelength; Q – the attenuation efficiency factor for single particles; l – the optical length of the probing; D – the particle diameter; $m = n + i\varphi$ – the complex refractive index of the particles material, n – the refractive index; φ – the absorption coefficient; $f(D)$ – the particle size distribution function.

Most of the unimodal particle distributions occurring in the disperse media physics as well as those characteristic of two-phase flows of various substances are described by the gamma distribution that takes the form:

$$f(D) = aD^\alpha \exp(-bD), \quad (2)$$

where a , α and b – the distribution parameters.

By introducing the notion of the averaged attenuation efficiency factor \bar{Q} in the form:

$$\bar{Q}(\lambda, m) = \frac{\int_0^\infty Q(\lambda, D, m) D^2 f(D) dD}{\int_0^\infty D^2 f(D) dD}, \quad (3)$$

and having replaced the calculated concentration C_n by the mass concentration C_m through

$$C_m = C_n \frac{\pi \rho_p}{6} \int_0^{\infty} D^3 f(D) dD, \quad (4)$$

we derive an expression for the optical thickness:

$$\tau_{\lambda_i} = \frac{1.5 C_m l \bar{Q}(\lambda, m)}{\rho_p D_{32}}, \quad (5)$$

where ρ_p - the material density of the particles; D_{32} - the mean volumetric-surface particle diameter that is calculated by the formula:

$$D_{32} = \frac{\int_0^{\infty} D^3 f(D) dD}{\int_0^{\infty} D^2 f(D) dD}, \quad (6)$$

The physical model of the method relies on the interaction between laser radiation and a polydisperse medium through the Mie mechanism and on the conservation of the invariance of the averaged attenuation efficiency factor with respect to a form of the particle size distribution function. The correctness of this assumption is governed by the fact that \bar{Q} is defined by integrals from $f(D)$ and, hence, \bar{Q} is insensitive to the behavior of $f(D)$ in the particle size range under consideration (Prishovalko & Naumenko, 1972).

The averaged attenuation efficiency factor under certain conditions is independent on a form of the particle size distribution function $f(D)$ but is determined by the mean volumetric-surface particle diameter D_{32} at a specified λ , $\bar{Q}_\lambda = f(D_{32})$, and is the most important feature determining the optical properties of polydisperse two-phase media.

The problem of estimating particle sizes by the present method reduces to measuring the optical density of a disperse medium at the two wavelengths λ_1 and λ_2 and to calculating averaged attenuation efficiency factors of laser radiation for the same wavelengths.

The relation of the experimentally measured optical thicknesses at the two wavelengths is equal to the relation of averaged attenuation efficiency factors, both representing the particle size function:

$$\frac{\tau_{\lambda_i}}{\tau_{\lambda_j}} = \frac{\bar{Q}_2(D_{32}, m, \lambda_i)}{\bar{Q}_1(D_{32}, m, \lambda_j)} = F_{ij}(D_{32}), \quad (7)$$

The measurement range of averaged particle sizes depends on selecting probe radiation wavelengths. Thus, at $\lambda_1 = 0.63$ and $\lambda_2 = 3.39 \mu\text{m}$ the D_{32} range is 0.5–4 μm .

The developed method employed the three wavelengths, $\lambda_1 = 0.63$, $\lambda_2 = 1.15$ and $\lambda_3 = 3.39$ μm , and the relations of the experimentally measured optical thicknesses at the three wavelengths, $\frac{\tau_{\lambda_2}}{\tau_{\lambda_1}}$, $\frac{\tau_{\lambda_3}}{\tau_{\lambda_1}}$, and $\frac{\tau_{\lambda_3}}{\tau_{\lambda_2}}$.

The averaged efficiency factors for each wavelength are calculated from precise formulae of the Mie theory which have the form of infinite weakly converging series obtained from the rigorous solution of the diffraction problem of electromagnetic fields on a sphere. The plots of the averaged efficiency factors $\bar{Q}_i(D_{32}, m, \lambda_i)$ versus the mean volumetric-surface diameter D_{32} are shown in Figure 1.

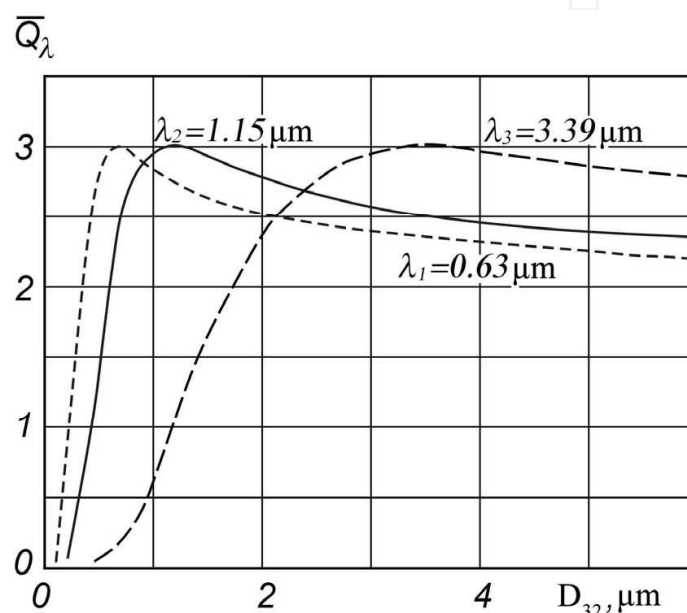


Fig. 1. The averaged attenuation efficiency factors of radiation \bar{Q} plotted against the mean volumetric-surface particle diameter D_{32}

The efficiency factors for single particles were calculated according to the Mie theory using a logarithmic derivative of the Riccati-Bessel function (Deyrmendzhan, 1997). The optical constants for oxide particles were taken from Gyvnak and Burch (1965).

Thus, D_{32} can be directly found from the experimentally measured τ_{λ_i} and calculated values of $F(D_{32})$. The particle concentration in the measuring zone is determined by the formula:

$$C_m = \frac{\tau_{\lambda_i} \rho_p D_{32}}{1.5 l \bar{Q}(\lambda_i, D_{32})}, \quad (8)$$

where $i = 1; 2; 3$ on the condition that the optical length of the probing is known or experimentally established, with the values of \bar{Q}_i being determined from the plots (Figure 1).

The practical realization of the multifrequency probing of two-phase media requires solving the problem of selecting radiation wavelengths at which the measurements should be

conducted, so that they could be informative with respect to the particle size range (Pavlenko et al., 2005).

The main condition for selecting λ_i during the method implementation is the explicit sensitivity of the dependence of \bar{Q} on the mean volumetric-surface particle diameter D_{32} , with the maximum of the functions $\bar{Q}(D_{32})$ being well-described by the formula:

$$D_{32}^{\circ} = \frac{\lambda}{\pi} \left(1 + \frac{4}{n^2 - 1} \right), \quad (9)$$

where D_{32}° - the mean particle size at which the function $\bar{Q}(D_{32})$ has an extremum; n - the aerosol particle refractive index.

Hence, when the variation range of the mean particles size of a medium under study is assigned *a priori*, the radiation wavelengths must be close to the values corresponding to the following expressions:

$$\lambda_1 = \pi D_{32}^{\min} \left(1 - \frac{4}{n^2 + 3} \right), \quad (10)$$

$$\lambda_2 = \pi D_{32}^{\max} \left(1 - \frac{4}{n^2 + 3} \right), \quad (11)$$

If λ_2 is lower than that determined by formula (11), the experiment will estimate the mean size of a small fraction of particles of a studied medium; and if λ_1 is greater that that determined by formula (10), the measured mean size will characterize a large fraction of the desired distribution.

For the selected wavelengths λ_1 and λ_2 , the dependence $\bar{Q}(D_{32})$ has been calculated and the relation $\bar{Q}_{\lambda_2} / \bar{Q}_{\lambda_1} = F(D_{32})$ determined. Table 2 lists data on the relations of the averaged attenuation efficiency factors of radiation $\bar{Q}_{\lambda_2} / \bar{Q}_{\lambda_1} = F(D_{32})$ for various wavelength pairs, depending on D_{32} , from which the limits of measuring the mean particle sizes are established.

In the given case, the maximal measurable particle size D_{32} will be determined by a value at which the function $F(D_{32})$ has a maximum. On the understanding that \bar{Q} is unambiguously dependent on D_{32} only in some interval of particle sizes, generally from zero up to the maximal value (Figure 1), and is an analog of the dependence of the efficiency factor Q on the particle diameter D for an arbitrary particle size distribution, $f(D)$, it follows that particles whose size exceeds D_{32}^{\max} out of the whole range of the disperse medium particle sizes are excluded from consideration. Here, we can introduce a notion of the active particle fraction in the distribution $f(D)$ for which there exists a strongly pronounced dependence of Q on D at different λ .

Thus, the laser measurement of the dispersiveness of two-phase media ascertains the mean size of the active particle fraction starting from zero up to some value that is dependent on the selection of λ_2 and at which the function $F(D_{32})$ reaches the maximum.

$D_{32}, \mu\text{m}$	F_{21}	F_{31}	F_{32}	$D_{32}, \mu\text{m}$	F_{21}	F_{31}	F_{32}
1.5	1.117	0.648	0.580	5.0	1.065	1.281	1.202
2.0	1.116	0.946	0.847	5.5	1.089	1.303	1.196
2.5	1.100	1.139	1.031	6.0	1.063	1.254	1.180
3.0	1.125	1.270	1.128	6.5	1.067	1.231	1.152
3.5	1.087	1.308	1.203	7.0	1.099	1.226	1.114
4.0	1.064	1.296	1.218	7.5	1.056	1.222	1.157
4.5	1.089	1.310	1.203	8.0	1.050	1.211	1.151

Table 2. The averaged attenuation efficiency factors for each wavelength: $\lambda_1 = 0.63 \mu\text{m}$, $\lambda_2 = 1.15 \mu\text{m}$, $\lambda_3 = 3.39 \mu\text{m}$

Based on the calculations of the dependences $\bar{Q}(D_{32})$ and $F(D_{32})$ for the corresponding wavelengths, the measurement ranges of D_{32} (D_{32}^{\min} , D_{32}^{\max}) and the active particle fraction range (D^{\min} , D^{\max}) of the studied distributions $f(D)$ were determined and are presented in Table 3.

$\lambda_1, \mu\text{m}$	$\lambda_2, \mu\text{m}$	$D_{32}^{\min}, \mu\text{m}$	$D_{32}^{\max}, \mu\text{m}$	$D^{\min}, \mu\text{m}$	$D^{\max}, \mu\text{m}$
0.63	1.15	0	1.5	0	1.5
0.63	3.39	0	3.5	0	4.0
1.15	3.39	0.1	3.6	0.1	4.0
0.63	5.30	0.8	6.5	0	8.0

Table 3. Ranges of the determinable active fractions of particles

The theory of the modified method of spectral transparency has been well elaborated so far for disperse media that are characterized by the unimodal particle size distribution. However, as it follows from the literature sources, in some cases like heterogeneous combustion, plasma spraying, local man-made aerodisperse systems, there is a possibility for a bimodal particle size distribution.

In order to expand the modified method of spectral transparency for investigating disperse systems of a bimodal particle size distribution, a mathematical model of calculating characteristics of the laser radiation attenuation by such media has been devised (Potapov & Pavlenko, 2000).

From the physical point of view, bimodal disperse media can correctly be described in the form of the following analytical dependence:

$$f(D) = aD^\alpha \exp(-bD^\beta) + c \exp[-p(D-q)^2], \quad (12)$$

where $a, c, b, p, q, \alpha, \beta$ - the distribution parameters. Dependence (12) is a sum of the generalized gamma distribution and normal distribution. The position of the first maximum is at point $D_0^{(1)} = \alpha/b$ and that of the second - $D_0^{(2)} = q$.

In the calculation of $\bar{Q}(D_{32})$, a series of D_{32} values and the corresponding distributions of $f(D)$ are preliminary assigned because the analytical dependence of D_{32} on the parameters of distribution (12) cannot be established.

What is important is to assign a form of the bimodal distribution, its determinative characteristics, and the variation mechanism of $f(D)$ when scanning the argument of the function $\bar{Q}(D_{32})$.

The following model of assigning $f(D)$ seems appropriate:

- the form of the bimodal particle size distribution function is determined by such characteristics as:

$$V = D_0^{(2)} - D_0^{(1)}, W = f[D_0^{(1)}] / f[D_0^{(2)}]; \quad (13)$$

- the variation of $f(D)$ upon scanning the argument of the function $\bar{Q}(D_{32})$ occurs on the condition that V and W remain constant.

Let the parameters α , β and q in equation (12) be represented as $\alpha = vk$, $b = 1$, $q = vk/b + V$, where $k = 1, 2, 3 \dots z$. From the condition of normalization and from formula (13) was a system of equations relative to the parameters a and b in formula (12) derived

$$a(k)E^{11} + b(k)E^{12} = E^{13}, \quad (14)$$

$$a(k)E^{21} + b(k)E^{22} = E^{23}, \quad (15)$$

where $E^{23} = 1$; $E^{13} = 0$, a E^{11} , E^{12} , E^{21} and E^{22} are calculated by the formulae:

$$E^{11} = (vk/b)^{vk} \exp(-vk) - W(V + vk/b^{vk} \exp[-(bV + vk)]), \quad (16)$$

$$E^{12} = \exp(-pV^2) - W, \quad (17)$$

$$E^{21} = \int_0^{\infty} D^{vk} \exp(-bD) dD, \quad (18)$$

$$E^{22} = \int_0^{\infty} \exp[-p(D - (vk/b - V))^2] dD, \quad (19)$$

The parameters $a(k)$ and $b(k)$ obtained from solving equations (14) - (15) are used to calculate $f_k(D)$, and $D_{32}(k)$. The found values of $f_k(D)$ are employed in software to compute \bar{Q} .

For the bimodality characteristics $V = 1 \div 2$ and $W = 0.25 \div 4$, $\bar{Q}(D_{32})$ was calculated from the suggested model. The character of the dependence $\bar{Q}(D_{32})$ for bimodal and unimodal

distributions was shown to be identical. In this case, the maximal value of \bar{Q} is kept at the corresponding value of D_{32} established from the theory:

$$D_{32} = \lambda \left[1 + 4 / (n^2 - 1) \right] / \pi . \quad (20)$$

This indicates that the model of calculating $\bar{Q}(D_{32})$ for bimodal particle size distributions may be regarded as correct.

When the modified method of spectral transparency was applied, the error in determining the particle sizes was established to grow due to the uncertainty of the particle size distribution class. To enhance the accuracy of the particle size determination, the probing of disperse media requires *a priori* information on a class of particle size distribution, either bimodal or unimodal, and requires the established invariance of \bar{Q} as a function of $f(D)$ within the limits of a certain distribution.

In the diagnostics of bimodal disperse media of a strongly pronounced functionality, when particle fractions are at a great distance from each other, it is possible to implement various mechanisms of the interaction between probing radiation and particles, on the basis of which the particle size of each separate fraction can be estimated. The bimodal distribution can be represented in the form:

$$f(D) = f_1(D) + f_2(D), \quad (21)$$

where $f_1(D)$ and $f_2(D)$ - the first and second functions that describe small and large particle fractions having the modal diameters $D_0^{(1)}$ and $D_0^{(2)}$ and the mean volumetric-surface diameters $D_{32}^{(1)}$ and $D_{32}^{(2)}$, respectively.

From the analysis of the range of the \bar{Q} dependence on D_{32} for various wavelengths, formulae for selecting the probe radiation wavelengths were derived:

$$\lambda_{i1} = D_{32}^{(i)} / \pi , \quad (22)$$

$$\lambda_{i2} = \lambda_{i1} \left(5 - D_{32}^{(i)} / 4 \right), \quad (23)$$

where $i = 1, 2$ - the number of particle size distribution functions.

With such a choice of wavelengths, there occurs a fractional interaction between the radiation and the polydisperse particles, and, in contrast to the common techniques, three scattering mechanisms are immediately brought about: Rayleigh scattering, Mie scattering, and scattering by large particles.

The interaction of the radiation of the wavelengths $\lambda = \lambda_{1j}$, where $j = 1, 2$ is the number of the radiation wavelengths needed for probing a separate fraction, with the first $f_1(D)$ and the second fractions $f_2(D)$ results in the Mie scattering and the scattering by large particles, respectively. When the radiation having the wavelengths $\lambda = \lambda_{2j}$ interacts with the first and second fractions, there occurs the Rayleigh scattering and Mie scattering, respectively.

Thus, when the radiation passes at the four wavelengths λ_{ij} through a bimodal disperse medium, the optical thicknesses τ are expressed by the following dependences:

$$\tau_{1j} = \frac{1,5l}{\rho_p} \left[M^{(1)} \frac{Q(\lambda_{1j})}{D_{32}^{(1)}} + M^{(2)} \frac{2}{D_{32}^{(2)}} \right], \quad (24)$$

$$\tau_{2j} = \frac{1,5l}{\rho_p} \left[M^{(1)} \frac{J}{\lambda_{2j}} + M^{(2)} \frac{Q(\lambda_{2j})}{D_{32}^{(2)}} \right], \quad (25)$$

where

$$J = \frac{24\pi n \phi}{(n^2 - \phi^2 + 2)^2 + 4n^2 \phi^2}. \quad (26)$$

The mean volumetric-surface diameters $D_{32}^{(i)}$ and particle mass concentrations $M^{(i)}$ for each separate fraction are determined from expressions (24) – (26).

To determine disperse characteristics of bimodal heterogeneous media of a strongly pronounced functionality, Ar, He-Ne and CO₂ lasers as well as collimated radiation-based semiconductor lasers can be employed.

To experimentally test the devised method of spectral transparency, the mean particle sizes of the combustion products produced from a model nozzle-free generator were estimated (Arkhipov et al. 2007).

The tests showed that the mean volumetric-surface diameter of the particles is 0.8–2.7 μm . Figure 2 illustrates typical experimental data on the dependences obtained.

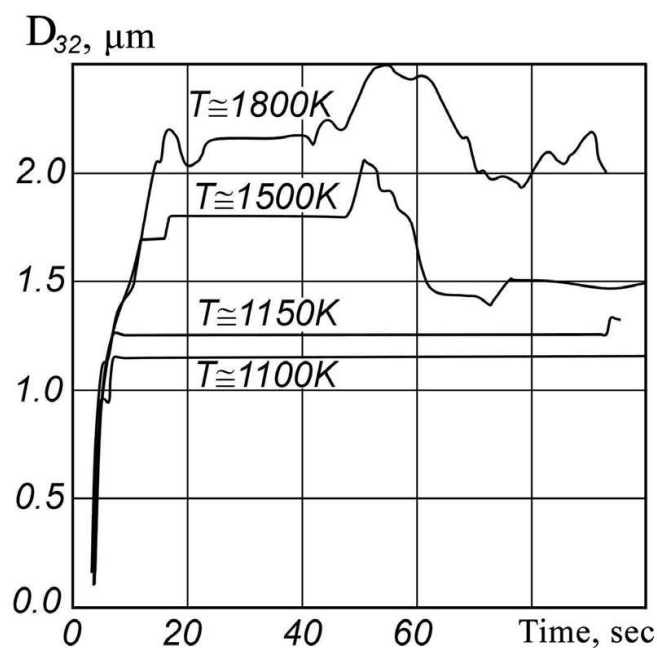


Fig. 2. Typical experimental data on the time dependences of D_{32} for various average temperatures in a combustion chamber

The nonmonotonic behavior of the dependences for higher temperatures is governed by a strong nonstationarity of intraballistic parameters under these conditions.

Data on the particle sizes are qualitatively consistent with the calculation results for particle size distribution spectra at the exit from the nozzle-free fire channel.

3. High-selective optical integral method of estimating the particle size distribution function

A new optical technique has been developed for determining the particle size distribution function in aerosol media with a particle size range of 0.1–5 μm and is based on the spectral transparency method.

The classical method of spectral transparency to estimate the particle dispersiveness relates to inverse problems of aerosol optics (Arkhipov, 1987). The stable solution of the problem of determining aerosol parameters by the spectral transparency method is possible if the transparency is ascertained over the whole wavelength range (Shifrin, 1971). However, nowadays devices can measure the spectral transparency coefficient only at several wavelengths or in some region of wavelengths without selectivity, which undoubtedly reduces accuracy and capabilities of the method (Shaikhatarov et al., 1986).

The method of spectral transparency relies on measuring the spectral transmission factor of optical radiation of a two-phase flow in some range of wavelengths. The initial equation for the method of spectral transparency is as follows (Van de Hulst, 1961):

$$I(\lambda, t) = I_0(\lambda) \exp \left[-\frac{\pi C_n(t) l(t)}{4} \int_0^\infty Q \left(\frac{\pi D}{\lambda}, m(\lambda) \right) D^2 f(D) dD \right], \quad (27)$$

where $I(\lambda, t)$ – the intensity of the radiation passed through the aerosol; $I_0(\lambda)$ – the probe radiation intensity; $C_n(t)$ – the calculated concentration of the aerosol condensed phase; $l(t)$ – the optical path length; $Q \left(\frac{\pi D}{\lambda}, m(\lambda) \right)$ – the attenuation efficiency factor of the probe radiation; $m(\lambda)$ – the complex refractory index of the aerosol condensed phase.

The problem of finding the aerosol particle diameter distribution $f(D)$ from expression (27) by the known radiation intensity values ($I(\lambda)$ and $I_0(\lambda)$) is incorrect. The said incorrectness is unavoidable for the spectral transparency method. It is suggested that the problem be solved using regularizing algorithms.

The regularizing algorithms are built in such a way as to attract additional *a priori* (with respect to the experiment on the basis of which the inverse problem is set) information on the desired function. With the aid of such information (details on smoothness of the desired solution, its monotonicity, convexity, pertain to the finitely parametric family, etc), such a solution is selected which is close to the true one in some specified sense. The regularizing algorithms allow a stable approximation to the true solution of an incorrect

problem, meaning that the approximate solution tends to the true one as the measurement error goes to zero.

One of the regularization ways is the parametrization technique. For the given situation, it will consist in the fact that a form of distribution function (2) is believed to be known *a priori*, in which case the parameters α and b are assigned by the coordinate-wise descent method, and the normalizing coefficient is to be found from the expression:

$$a = \left[\int_{D_{\min}}^{D_{\max}} D^\alpha \exp(-bD) dD \right]^{-1}, \quad (28)$$

where D_{\min} and D_{\max} are the minimal and maximal diameters of the particles present in a medium under examination, respectively. Gamma distribution (2) for describing the particle size distribution was chosen in view of its universality as applied to aerosols, with one mechanism of producing a disperse phase (Arkhipov et al., 2006). The attenuation efficiency factor of the probe radiation ($Q\left(\frac{\pi D}{\lambda}, m(\lambda)\right)$) is calculated by the formula using specified parameters of the distribution function:

$$Q\left(\frac{\pi D}{\lambda}, m(\lambda)\right) = \frac{2}{\left(\frac{\pi D}{\lambda}\right)^2} \sum_{n=1}^{\infty} (2n+1) \operatorname{Re}(a_n + b_n), \quad (29)$$

where a_n and b_n are the Mie coefficients and are calculated by the formula:

$$a_n\left(\frac{\pi D}{\lambda}, m(\lambda)\right) = \frac{\left[\frac{A_n\left(\frac{\pi D m(\lambda)}{\lambda}\right)}{m(\lambda)} + \frac{n}{\left(\frac{\pi D}{\lambda}\right)} \right] \operatorname{Re}\left[\xi_n\left(\frac{\pi D}{\lambda}\right)\right] - \operatorname{Re}\left[\xi_{n-1}\left(\frac{\pi D}{\lambda}\right)\right]}{\left[\frac{A_n\left(\frac{\pi D m(\lambda)}{\lambda}\right)}{m(\lambda)} + \frac{n}{\left(\frac{\pi D}{\lambda}\right)} \right] \xi_n\left(\frac{\pi D}{\lambda}\right) - \xi_{n-1}\left(\frac{\pi D}{\lambda}\right)}, \quad (30)$$

$$b_n\left(\frac{\pi D}{\lambda}, m(\lambda)\right) = \frac{\left[m(\lambda) A_n\left(\frac{\pi D m(\lambda)}{\lambda}\right) + \frac{n}{\left(\frac{\pi D}{\lambda}\right)} \right] \operatorname{Re}\left[\xi_n\left(\frac{\pi D}{\lambda}\right)\right] - \operatorname{Re}\left[\xi_{n-1}\left(\frac{\pi D}{\lambda}\right)\right]}{\left[m(\lambda) A_n\left(\frac{\pi D m(\lambda)}{\lambda}\right) + \frac{n}{\left(\frac{\pi D}{\lambda}\right)} \right] \xi_n\left(\frac{\pi D}{\lambda}\right) - \xi_{n-1}\left(\frac{\pi D}{\lambda}\right)}, \quad (31)$$

where A_n and ξ_n are in recurrence relationships:

$$\xi_n \left(\frac{\pi D}{\lambda} \right) = \frac{2n-1}{\left(\frac{\pi D}{\lambda} \right)} \xi_{n-1} \left(\frac{\pi D}{\lambda} \right) - \xi_{n-2} \left(\frac{\pi D}{\lambda} \right), \quad (32)$$

$$\xi_0 \left(\frac{\pi D}{\lambda} \right) = \sin \left(\frac{\pi D}{\lambda} \right) + i \cos \left(\frac{\pi D}{\lambda} \right), \quad (33)$$

$$\xi_{-1} \left(\frac{\pi D}{\lambda} \right) = \cos \left(\frac{\pi D}{\lambda} \right) - i \sin \left(\frac{\pi D}{\lambda} \right), \quad (34)$$

$$A_n \left(\frac{\pi D m(\lambda)}{\lambda} \right) = -\frac{n}{\left(\frac{\pi D m(\lambda)}{\lambda} \right)} + \left[\frac{n}{\left(\frac{\pi D m(\lambda)}{\lambda} \right)} - A_{n-1} \left(\frac{\pi D m(\lambda)}{\lambda} \right) \right]^{-1}, \quad (35)$$

$$A_0 \left(\frac{\pi D m(\lambda)}{\lambda} \right) = \operatorname{ctg} \left(\frac{\pi D m(\lambda)}{\lambda} \right). \quad (36)$$

The limit of summation in expression (29) comes when the condition is fulfilled:

$$\left[\sum_{n=1}^N (2n+1) \operatorname{Re}(a_n + b_n) \right] \cdot 10^{-8} > (2(N+1)+1) \operatorname{Re}(a_{N+1} + b_{N+1}). \quad (37)$$

To solve the problem, the spectral transparency coefficient is used as experimental information and is calculated by the formula:

$$\tau_{\lambda}^e(t) = \ln \frac{I_0(\lambda)}{I(\lambda, t)}. \quad (38)$$

Afterwards, there is found a relation of the spectral transparency coefficients obtained from experiments for some wavelengths λ_1 and λ_2 :

$$k_e(t) = \frac{\tau_{\lambda_1}^e(t)}{\tau_{\lambda_2}^e(t)}. \quad (39)$$

Then, a relation of the theoretically obtained coefficients of spectral transparency for various distribution functions (2) is calculated, in accordance with equation (27) for the wavelengths λ_1 and λ_2 , by the formula:

$$k_d(t) = \frac{\tau_{\lambda_1}^d(t)}{\tau_{\lambda_2}^d(t)} = \frac{\int_{D_{\min}}^{D_{\max}} Q \left(\frac{\pi D}{\lambda_1}, m(\lambda) \right) D^2 f(D) dD}{\int_{D_{\min}}^{D_{\max}} Q \left(\frac{\pi D}{\lambda_2}, m(\lambda) \right) D^2 f(D) dD}. \quad (40)$$

The cumulative departure of the experimental data $k_e(t)$ from the theoretical $k_d(t)$ is further calculated for all the wavelengths used. In addition, mathematical studies showed that the selection method for pairs of the wavelengths λ_1 and λ_2 has no affect on the accuracy and performance stability of the algorithm suggested and, hence, any selection method can be employed. The comparison of the relations of the spectral transparency coefficients but not their absolute values was undertaken to get rid of the constant factor before the integral sign in expression (27) when calculating theoretical values of the transmission factors of a medium under study (40).

The final step is selecting such a form of the particle size distribution function wherein the departure of the experimental data from the theoretical is minimal.

The direct problem of estimating the spectral coefficient of the probe radiation attenuation for various parameters of the distribution function can thus be solved by the numerical methods.

The optical path length (l) of the probe radiation (say, with high-speed video shooting (Titov & Muravlev, 2008)) in a studied aerosol is then determined, and the mass concentration of the aerosol dispersed phase is calculated by the formula:

$$C_m(t) = \frac{\tau_\lambda^e(t) \rho_p D_{32}}{1.5l(t) \bar{Q}\left(\frac{\pi D}{\lambda}, m(\lambda)\right)}, \quad (41)$$

$$\bar{Q}\left(\frac{\pi D}{\lambda}, m(\lambda)\right) = \frac{\int_{D_{\min}}^{D_{\max}} Q\left(\frac{\pi D}{\lambda}, m(\lambda)\right) D^2 f(D) dD}{\int_{D_{\min}}^{D_{\max}} D^2 f(D) dD}. \quad (42)$$

To verify the operability of the method devised, an experiment to measure the attenuation of the optical radiation by a suspension of chemically pure submicron Al_2O_3 powder in distilled water was performed. Aluminum oxide was chosen because empirical dependences of refractive and absorption indices on probe radiation wavelength for this substance are known (Dombrovskiy, 1982). Neglecting the dependence and using constants as refractive and absorption indices for all the wavelengths was shown by preliminary experiments to result in errors.

The suspended aluminum oxide was exposed to ultrasound in order to grind the resultant agglomerates, following which the whole was placed into a glass cuvette for examination. Prior to measurement, the cuvette was left to stand undisturbed to settle down ungrindable agglomerates. The cuvette that is part of the measuring complex is displayed in Figure 3. The numbers in Figure 3 denote: 1 - glare shield, 2 - collimator outlet, 3 - cuvette, 4 - condenser, 5 - optical waveguide, 6 - direction of optical radiation passage. All the dimensions in Figure 3 are given in millimeters. The optical radiation path length in the medium studied (distance between the inner surfaces of the cuvette glasses) was 5.075 mm.

Before measuring the radiation transmission through the cuvette with suspended aluminum oxide, the radiation transmission through the cuvette filled with pure distilled water was estimated. The transmission spectrum of the cuvette with pure distilled water was used as the reference; it is necessary for all variations of the transmission spectrum of the suspension with respect to the reference spectrum to be caused only by the action of aluminum oxide nanopowder. The reference spectrum and the transmission spectrum of the studied suspension are shown in Figure 4.

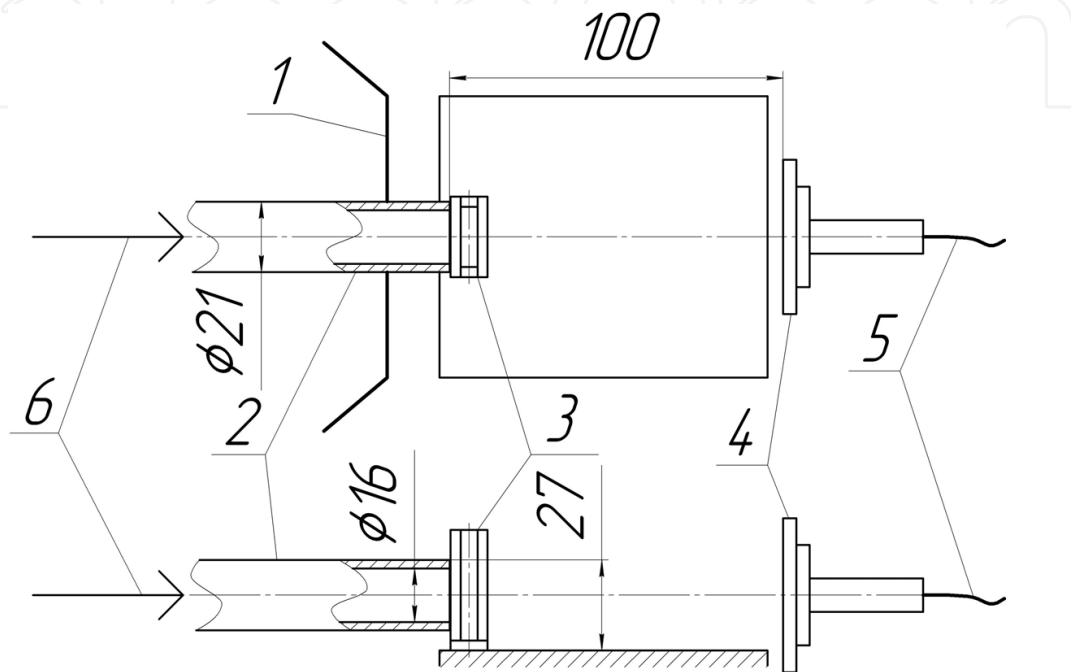


Fig. 3. The cuvette compartment of the measuring complex

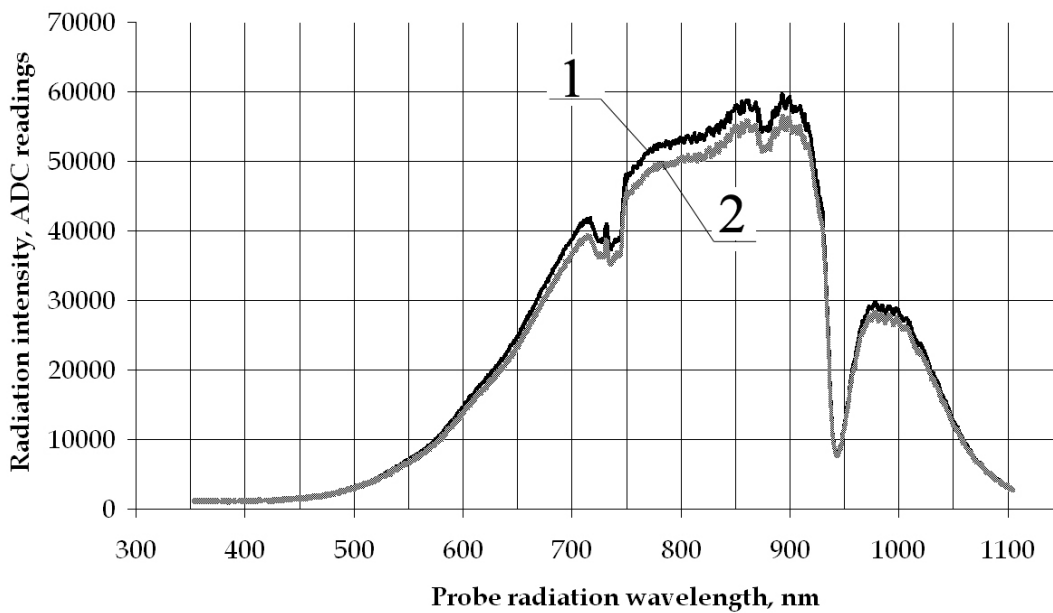


Fig. 4. The optical radiation transmission spectra: 1 - cuvette transmission spectrum with pure distilled water; 2 - cuvette transmission spectrum with Al₂O₃ suspension

From the spectral data presented was the spectral transparency coefficient calculated by formula (38); the resultant dependence of the spectral transparency coefficient on the wavelength is displayed in Figure 5. The moving average method was applied to the dependence shown in Figure 5 in order to eliminate high-frequency noises, resulting in dependence no.1 in Figure 6. The theoretical dependence of the spectral transparency coefficient on the probe radiation wavelength is no.2 in Figure 6, its difference from the experimental data appearing to be minimal.

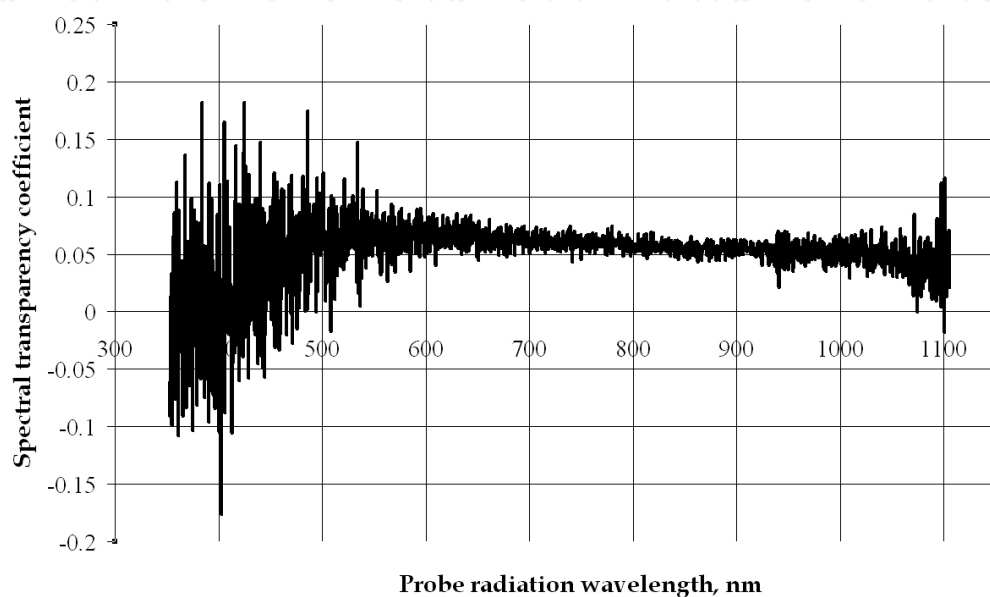


Fig. 5. Experimental spectral transparency coefficient

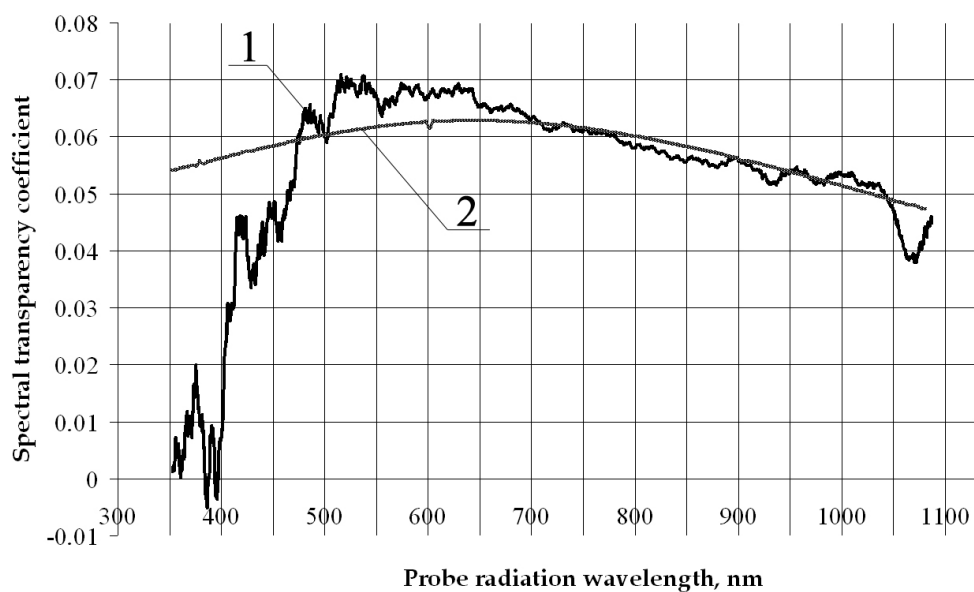


Fig. 6. Experimental and theoretical dependences of the spectral transparency coefficients on the probe radiation wavelength: 1 - experiment; 2 - calculation

The strong difference of the experimental data from the theoretical in the region of wavelengths up to 480 nm is due to the low-level wanted signal therein, as is well illustrated

in Figure 4, which nearly coincides with the noise value. This can also be seen from the untreated dependence of the spectral transparency coefficient on the wavelength in Figure 5. This discrepancy can therefore be considered acceptable since instrumental implementation peculiarities are concerned regarding the measurement of optical radiation attenuation, and it does not characterize the algorithm applied.

The found theoretical dependence of the spectral transparency coefficient on the wavelength (curve 2, Figure 6) is consistent with the particle size distribution function shown in Figure 7.

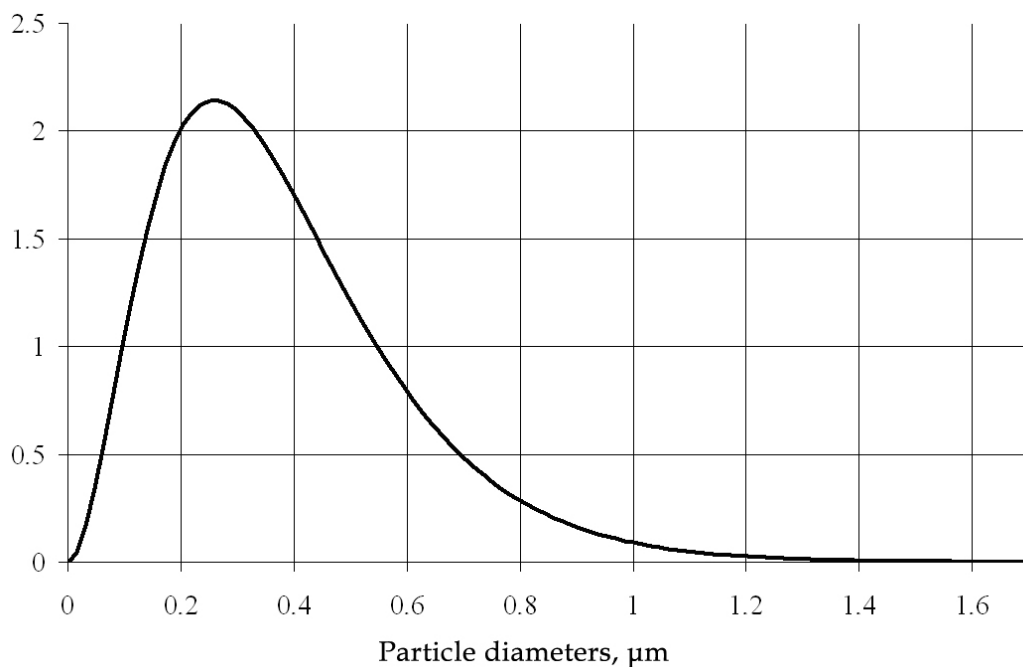


Fig. 7. The restored Al_2O_3 particle size distribution function

The particle size distribution function obtained (Figure 7) is in good agreement with the known data on the aluminum oxide nanopowder studied.

4. Modified method of small-angle scattering

To investigate the aerosol genesis from 2 to 100 μm , a method based on estimating disperse parameters of aerosols from the measured scattered radiation passed through a studied volume has been devised.

The method consists in finding the aerosol particle size range from the measured scattering indicatrix, by means of searching the corresponding parameters of the distribution function. Gamma distribution (2) was accepted as the reference function (Arkhipov, 1987).

Laser beam LS (Figure 8) propagates through a scattering layer with boundaries "1" and "2" to produce some illuminance on plane Y. The distance between the laser and the first boundary of the layer is l_1 . The aerosol cloud particles present in the beam scatter radiation. As a consequence, the irradiance of plane Y is determined not only by the direct beam attenuated due to absorption and scattering, but also by the radiation scattered by the particles.

On the assumption of the uniform distributions of concentration and particles sizes in the aerosol cloud, the equation for scattered radiation flux coming on plane Y has the following form:

$$I(y) = \frac{\pi S}{4} \int_0^z [I_0(x) B(x, y) F(x)] dx. \quad (43)$$

where $F(x) = \int_0^\infty Q_s(D, \theta(x)) D^2 f(D) dD$; $I_0(x) = I_0 \exp[-x C_n Q_{ext}]$ - the intensity of the radiation falling on point x ; I_0 - the initial radiation intensity; x - the distance between boundary "1" of the scattering layer and point P ; Q_{ext} - the attenuation coefficient.

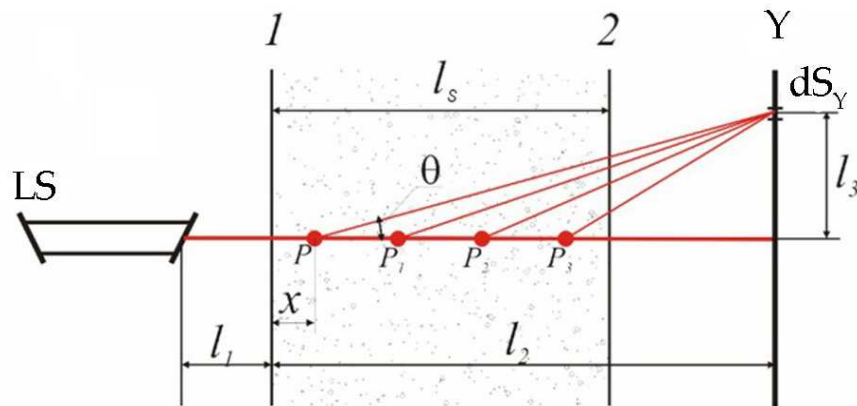


Fig. 8. Diagram of interaction between radiation and aerosol

The radiation scattered from a single particle in the small-angle region under the assumption that the particles are spherical is defined as an analytical dependence in the following form:

$$Q_s(\rho, \theta) = \frac{\rho^2}{4\pi} \cdot \left[\frac{2J_1(\theta\rho)}{\theta\rho} \right]^2, \quad (44)$$

where $\rho = \frac{\pi D}{\lambda}$ - the diffraction parameter (Mie parameter); θ - the radiation scattering angle; $J_1(\theta\rho)$ - the first-order Bessel function of the first kind.

The multiplier $B(x)$ that takes into account the scattered radiation attenuation pursuant to the Bugar law is defined by the relation:

$$B(x, y) = \exp \left[-Q_{ext} \frac{z - x}{\cos \theta(x, y)} \right], \quad (45)$$

where $\theta(x, y) = \arctg(y / (l_2 - x))$; $y = l_3$.

The estimation of $f(D)$ from the measured scattering indicatrix $I_e(y)$ reduces to searching the parameters $\{\alpha, b\}$ of distribution (2) and calculating the functional:

$$\Omega = \min_{a,b} \left\{ \sum_{i=1}^n |I_e(y_i) - I(y_i)| \right\}, \quad (46)$$

where $I_e(y_i)$ ($i=1, 2, \dots, n$) - the measured values of the scattering indicatrix for discrete values of the detector positions; $I(y_i)$ - the values calculated from (43).

It is possible to restore the droplet size distribution function with a sufficient accuracy if the condition is fulfilled (Gritsenko & Petrov, 1979; Belov et al., 1984):

$$\ln \frac{I_0}{I} \leq 1.5, \quad (47)$$

where I_0, I - the illuminance in the central beam before and after its passing through the scattering volume.

To implement the title method, a laser setup has been assembled which comprises (Figure 9): a 1 m³ measuring chamber; a radiator – HeNe laser with 0.632 μm wavelength and 5 mW power; a recording unit consisted of 8 photodiodes placed on the same array; a measuring 8-channel amplifier; ADC and PC; software to record and process measurement information in order to determine calculated and mass functions of particle size distribution, mean volumetric-surface diameter, and aerosol particles concentration.

The laser radiation is 90° angle oriented toward one of the volume faces, 80 Hz frequency modulated, and directed through a scattering medium.

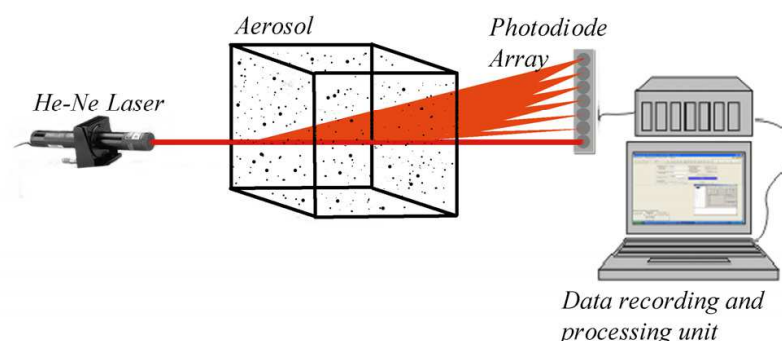


Fig. 9. The laser setup diagram

The optical radiation flux scattered at different angles is recorded by the photodiode array that is located in the plane perpendicular to the laser beam. The photodiode array enables recording the scattered radiation at angles of 0.3–20° relative to the laser beam.

The optical path length is estimated with the aid of a video camera or is set to a fixed value equal to a measuring volume for a steady-state generation process of a two-phase flow.

The aluminum powder measurement results obtained using the setup are collected in Table 4; Figure 10 shows mass functions of the particle size distribution.

Measurement	Distribution coefficient α	Distribution coefficient b	$D_{32}, \mu\text{m}$	$D_{43}, \mu\text{m}$
1	1.14	0.7	5.91	7.3
2	0.3533	0.55	6.09	7.91
3	0.53	0.53	6.66	8.54
4	1.24	0.64	6.6	8.2
5	1.1	0.7	5.8	7.2

Table 4. The laser method study results for the fine aluminum powder

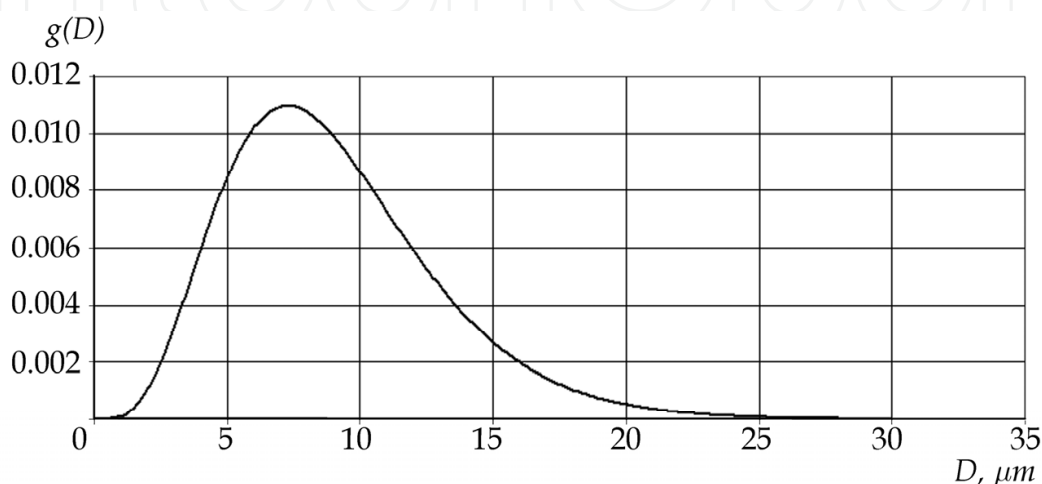


Fig. 10. The mass particle size distribution for the fine aluminum powder

The calculated distribution function can readily be converted into the mass distribution function by the formula (Arkhipov et al., 2006):

$$g(D) = \frac{m}{m_0} f(D), \quad (48)$$

where m - the weight of the particles of size D ; $m_{10} = \int_0^{\infty} mf(D)dD$.

The spread of the aluminum powder dispersiveness estimation results obtained using different methods is not greater than 15%, as demonstrated in Table 5.

An aerosol water cloud produced by pulsed generation was also studied. The results for water and an aqueous glycerol solution are given in Figures 11–13.

	Fine aluminum powder	
	$D_{32}, \mu\text{m}$	$D_{43}, \mu\text{m}$
Sieve analysis	7.2	8.3
Microscope	5.7	6.44
Modified method of small-angle scattering	6.2	7.45

Table 5. Comparison of the results of different methods

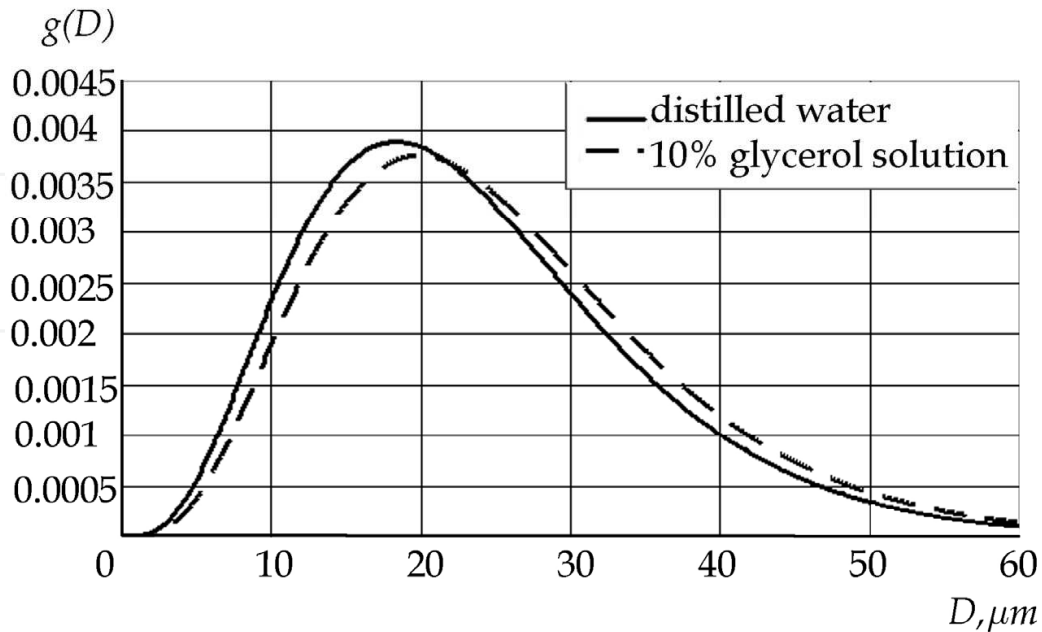


Fig. 11. Mass droplet distribution after spraying (time, 1 s)

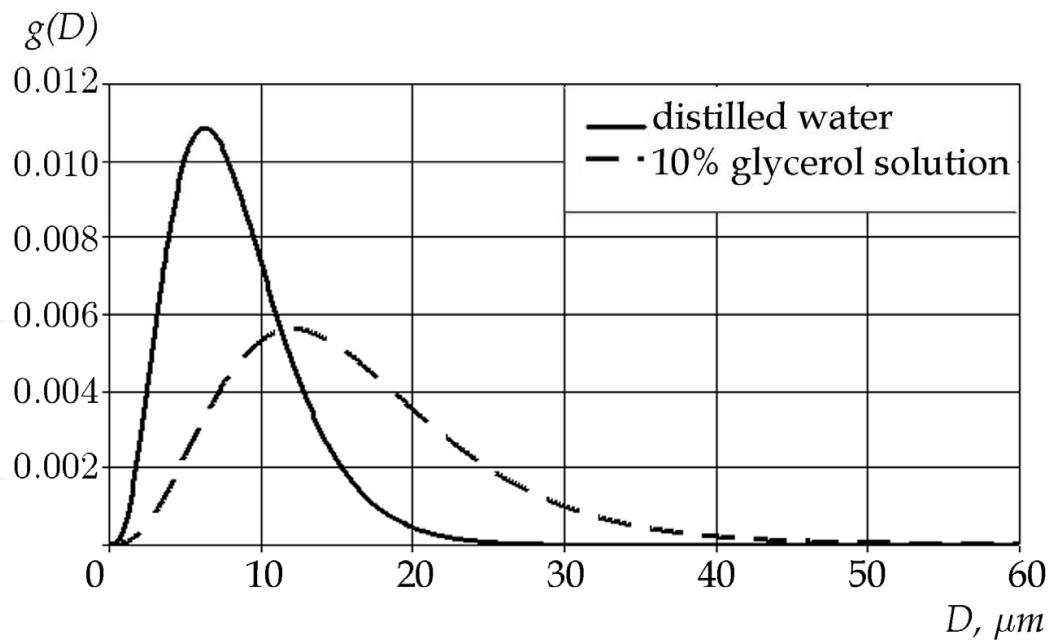


Fig. 12. Mass droplet distribution after spraying (time, 6 s)

The modified small-angle scattering method developed makes it possible to restore the particle size distribution function even from three measured points of the scattering indicatrix.

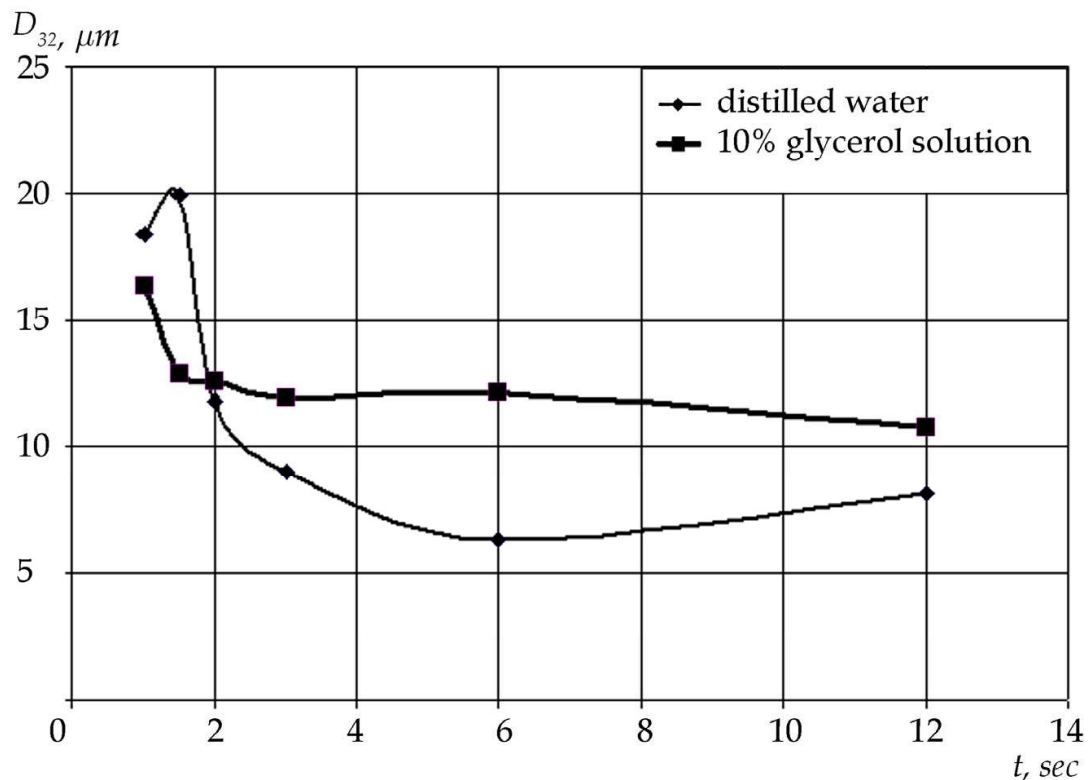


Fig. 13. The change in the mean size D_{32} of water and 10% glycerol solution droplets as a function of the aerosol cloud generation time

5. Conclusion

The optical diagnostics methods for heterogeneous flows have been reviewed and analyzed as the most promising with respect to measuring the dispersiveness and concentration of aerosol particles in dynamics, including the cases of high-velocity flows, significant background illuminance, and similar phenomena accompanying technological processes and affecting measuring instrumentation.

The authors have suggested and implemented a modified method of spectral transparency for estimating the aerosol dispersiveness, which is distinct both in simplicity of instrumental implementation and in possibility of diagnosing two-phase flows of a high optical density.

A new method of determining the particle size distribution function has been developed and is based on the classical method of spectral transparency using information on the probe radiation attenuation in a wide range of wavelengths; the operability of the method has been verified.

The inverse problem of aerosol optics has mathematically been solved for the small-angle scattering method in a part of results processing in order to eliminate incorrect solutions when restoring the particles size distribution function; the possibility of studying the dynamics of generation and propagation of aerosols using the algorithm suggested has been demonstrated.

The developed measuring complex employs data recording and processing algorithms obtained for the first time and combines the modified method of spectral transparency, the high-selective optical integral method of estimating the particle size distribution function, and the modified method of small-angle scattering. The combined application of the methods devised makes it possible to estimate disperse parameters of aerosol media of any nature and of a wide particle size range (0.1–100 μm) under conditions of their high-velocity genesis with a high time resolution. The measuring complex permits studying the genesis of two-phase flows and evaluating the effects on the fractional composition by such processes as particle coagulation, sedimentation, and evaporation.

6. References

- Arkhipov, V. (1987). Laser diagnostics methods of heterogeneous flows (in Russian), Tomsk University Press, Tomsk
- Arkhipov, V.; Akhmadeev, I.; Bondarchuk, S.; Vorozhtsov, B.; Pavlenko, A. & Potapov, M. (2007). A modified method of spectral transparency to measure aerosol dispersiveness (in Russian), *Atmospheric and Oceanic Optics*, Vol. 20, No. 1, pp. 48–52, ISSN 0869–5695
- Arkhipov, V.; Bondarchuk, S.; Korotkikh, A. & Lerner, M. (2006). Production technology and disperse characteristics of aluminum nanopowders (in Russian). *Gornyi Zhurnal. Special Issue. "Nonferrous Metals"*, No.4, pp. 58–64, ISSN 0372–2929
- Belov, V.; Borovoi, A. & Volkov, S. (1984). On the small-angle method under single and multiple scattering (in Russian). *Izvestia AN SSSR Fizika Atmosfery i Okeana*, Vol.20, No.3, pp.323–327
- Deyrmendzhan, D. (1997). Electromagnetic radiation scattering by spherical polydisperse particles (in Russian), Mir, Moscow
- Dombrovskiy, L. (1982). On a possibility of determining the dispersed composition of a two-phase flow by small-angle light scattering (in Russian), *Teplofizika Vysokikh Temperatur*, No.3, pp.549–557, ISSN 0040–3644
- Gritsenko, A. & Petrov, G. (1979). On the role of the multiple scattering in the inverse optics problems of coarse-dispersed aerosols (in Russian). *Optics and Spectroscopy*, Vol.46, No.2, pp.346–349, ISSN 0030–4034
- Gyvnač, D. & Burch, D. (1965). Optical and infrared properties of Al_2O_3 at elevated temperatures. *Journal of Optical Society of America*, Vol. 55, No.6, pp. 625–629
- Pavlenko, A.; Arkhipov, V.; Vorozhtsov, B.; Ahmadeev, I. & Potapov, M. (2005). Informative radiation wavelengths under laser diagnostics of aerosol media (in Russian), *XII Joint International Symposium "Atmospheric and Oceanic Optics. Atmospheric physics"*, Tomsk: IAO SB RAS, pp. 148
- Potapov, M. & Pavlenko, A. (2000). A mathematical model of calculating characteristics of the laser radiation attenuation for bimodal media (in Russian), *Proceedings of the 1st All-Russian conference "Measurements, automation and simulation in industry and scientific research"*, Biysk, pp. 135–139, ISSN 2223–2656
- Prishivalo, A. & Naumenko, E. (1972). The light scattering by spherical particles and polydisperse media (in Russian), IF AN BSSR, Minsk
- Shaikhatarov, K.; Lapshin, A.; Stolyarov, A. & lapshina, T. (1986). Disperse media photometer, Pat. SU 1435955 A1 G 01J 1/44

- Shifrin, K. (1971). The study of substance properties from single scattering (in Russian), In: *Theoretical and Applied Problems of Light Scattering*, B.I. Stepanov, A.P. Ivanov, (Ed.), pp. 228–244, Nauka i Tekhnika, Minsk
- Titov, S. & Muravlev, E. (2008). The use of a Videosprint/C/G4 digital camera in the studies of dynamic processes (in Russian), *All-Russian Conference "Perspectives of Designing and Applying High-energy Condensed Materials"*, pp. 173–179, ISBN 978-5-9257-0134-8, Biysk, Russia, 25-26 Sep 2008
- Van de Hulst, G. (1961). *Light scattering by fine particles*, Moscow
- Vorozhtsov, B.; Potapov, M.; Pavlenko, A.; Lushev, V.; Galenko, Yu. & Khrustalev, Yu. (1997). A multifrequency laser measuring complex of monitoring atmospheric and industrial aerosols (in Russian), *Atmospheric and Oceanic Optics*, Vol. 10, No. 7, pp. 928-832, ISSN 0869-5695
- Zuyev, E.; Kaul, B.; Samokhvalov, I.; Kirkov, K. & Tsanev, V. (1986). *The laser probing of industrial aerosols* (in Russian), Nauka, Novosibirsk

IntechOpen



Photodetectors

Edited by Dr. Sanka Gateva

ISBN 978-953-51-0358-5

Hard cover, 460 pages

Publisher InTech

Published online 23, March, 2012

Published in print edition March, 2012

In this book some recent advances in development of photodetectors and photodetection systems for specific applications are included. In the first section of the book nine different types of photodetectors and their characteristics are presented. Next, some theoretical aspects and simulations are discussed. The last eight chapters are devoted to the development of photodetection systems for imaging, particle size analysis, transfers of time, measurement of vibrations, magnetic field, polarization of light, and particle energy. The book is addressed to students, engineers, and researchers working in the field of photonics and advanced technologies.

How to reference

In order to correctly reference this scholarly work, feel free to copy and paste the following:

Olga Kudryashova, Anatoly Pavlenko, Boris Vorozhtsov, Sergey Titov, Vladimir Arkhipov, Sergey Bondarchuk, Eugeny Maksimenko, Igor Akhmadeev and Eugeny Muravlev (2012). Remote Optical Diagnostics of Nonstationary Aerosol Media in a Wide Range of Particle Sizes, Photodetectors, Dr. Sanka Gateva (Ed.), ISBN: 978-953-51-0358-5, InTech, Available from: <http://www.intechopen.com/books/photodetectors/remote-optical-diagnostics-of-nonstationary-aerosol-media-in-a-wide-range-of-particle-sizes>

INTECH
open science | open minds

InTech Europe

University Campus STeP Ri
Slavka Krautzeka 83/A
51000 Rijeka, Croatia
Phone: +385 (51) 770 447
Fax: +385 (51) 686 166
www.intechopen.com

InTech China

Unit 405, Office Block, Hotel Equatorial Shanghai
No.65, Yan An Road (West), Shanghai, 200040, China
中国上海市延安西路65号上海国际贵都大饭店办公楼405单元
Phone: +86-21-62489820
Fax: +86-21-62489821

© 2012 The Author(s). Licensee IntechOpen. This is an open access article distributed under the terms of the [Creative Commons Attribution 3.0 License](#), which permits unrestricted use, distribution, and reproduction in any medium, provided the original work is properly cited.

IntechOpen

IntechOpen